



Published in final edited form as:

Nat Commun. ; 5: 5155. doi:10.1038/ncomms6155.

SLO-2 potassium channel is an important regulator of neurotransmitter release in *Caenorhabditis elegans*

Ping Liu, Bojun Chen, and Zhao-Wen Wang*

Department of Neuroscience, University of Connecticut Health Center, Farmington, CT 06001, USA

Abstract

Slo2 channels are prominent K⁺ channels in mammalian neurons but their physiological functions are not well understood. Here we investigate physiological functions and regulation of the *C. elegans* homologue SLO-2 in motor neurons through electrophysiological analyses of wild-type and mutant worms. We find that SLO-2 is the primary K⁺ channel conducting delayed outward current in cholinergic motor neurons, and one of two K⁺ channels with this function in GABAergic motor neurons. Loss-of-function mutation of *slo-2* increases the duration and charge transfer rate of spontaneous postsynaptic current bursts at the neuromuscular junction, which are physiological signals used by motor neurons to control muscle cells, without altering postsynaptic receptor sensitivity. SLO-2 activity in motor neurons depends on Ca²⁺ entry through EGL-19, an L-type voltage-gated Ca²⁺ channel (Ca_v1), but not on other proteins implicated in either Ca²⁺ entry or intracellular Ca²⁺ release. Thus, SLO-2 is functionally coupled with Ca_v1 and regulates neurotransmitter release.

Introduction

A major function of K⁺ channels in neurons is to regulate the release of neurotransmitters. A variety of K⁺ channels have been found to have this physiological function, including the Ca²⁺- and voltage-gated high-conductance K⁺ channel Slo1 (BK channel)¹. Recent studies show that two other large-conductance K⁺ channels of the Slo gene family, Slo2.2 (*Slack*) and Slo2.1/*Slick*, are also broadly expressed in the nervous system^{2,3} (www.brain-map.org). Slo2.2 plays major roles in conducting delayed outward current in diverse mammalian central neurons examined⁴⁻⁶. Suppression of Slo2.2 expression may enhance neuron excitability and pain sensitivity⁷⁻⁹. A strong link has been established between mutations of KCNT1 (gene encoding Slo2.2) and epileptic disorders¹⁰⁻¹⁴. These observations suggest that Slo2 channels in neurons may play important physiological roles. However, studies on

Users may view, print, copy, and download text and data-mine the content in such documents, for the purposes of academic research, subject always to the full Conditions of use:http://www.nature.com/authors/editorial_policies/license.html#terms

*Correspondence: Zhao-Wen Wang, Department of Neuroscience, University of Connecticut Health Center, 263 Farmington Avenue, Farmington, CT 06030-3401, zwwang@uchc.edu.

Author Contribution

PL and ZWW conceived the project. PL and BC performed the experiments. ZWW and PL wrote the manuscript.

The authors declare no competing financial interests.

Slo2 channels with either knockout preparations or specific blockers are lacking, which makes it difficult to precisely define their physiological roles.

Slo2 channels are activated by membrane depolarization and cytosolic Cl^- and Na^+ ^{15, 16}. They are considered to be the molecular entity of Na^+ -activated K^+ (K_{Na}) channels observed in a variety of cells^{17, 18}. One conundrum about K_{Na} channels is that a concentration of Na^+ much higher than what could possibly occur in the bulk cytoplasm under physiological conditions is required for significant channel activation^{17, 18} although these channels appear to be active under physiological conditions^{5, 19–21}. Recent studies of Slo2.2 suggest that Na^+ entry, through either a persistent tetrodotoxin-sensitive channel(s) of unknown molecular identity^{4–6} or AMPA receptors²², may produce Na^+ microdomains necessary for K_{Na} channel activation.

C. elegans has a single Slo2 orthologue known as SLO-2, which is also gated by voltage and intracellular Cl^- but differs from mammalian Slo2 in that intracellular Ca^{2+} instead of Na^+ activates the channel^{23, 24}. The $[\text{Ca}^{2+}]$ required for *C. elegans* SLO-2 activation²³ is also much higher than what could possibly occur in the bulk cytoplasm under physiological condition. It is unknown whether Ca^{2+} entry plays an analogous role in SLO-2 activation as does Na^+ entry for Slo2 activation. In *C. elegans* body-wall muscle, SLO-2 conducts approximately 70% of the total delayed outward current; and *slo-2* loss-of-function (*lf*) mutation results in a more depolarized resting membrane potential, a wider action potential waveform, and a smaller amplitude of afterhyperpolarization, suggesting that SLO-2 plays important roles in controlling muscle function²⁵. Although SLO-2 is also expressed in the nervous system^{23, 26}, its physiological roles in neurons are unknown.

C. elegans neuromuscular junction (NMJ) is often used as a model synapse for analyzing the roles of proteins in synaptic transmission. However, electrophysiological analyses of this synapse have been limited to recording postsynaptic current (PSC) from body-wall muscle cells. To our knowledge, there has been no report on whole-cell voltage- and current-clamp recordings from *C. elegans* motor neurons. In the present study, we successfully performed electrophysiological recordings of motor neurons, and combined the electrophysiological data with PSCs recorded from body-wall muscle cells to assess physiological roles of SLO-2 in motor neurons. Our results suggest that SLO-2 is a major contributor to delayed outward current in motor neurons with its activity dependent on Ca^{2+} entry through a L-type voltage-gated Ca^{2+} channel (VGCC), and that SLO-2 controls the strength of synaptic transmission by regulating the duration and charge transfer rate of PSC bursts, which are used by motor neurons to control body-wall muscle²⁷. The prominent roles of Slo2/SLO-2 in conducting delayed outward current in both mammalian and nematode neurons suggest that these channels likely have important and conserved physiological functions.

Results

SLO-2 is important to outward current in motor neurons

Motor neurons controlling *C. elegans* body-wall muscle include three major classes: A, B and D. The A and B classes mediate backward and forward movements, respectively, and contract muscle by releasing acetylcholine (ACh), whereas the D class relaxes muscle by

releasing GABA^{28, 29}. To investigate physiological roles of SLO-2 in motor neurons, we chose VA5, VB6 and VD5 (the letter “V” stands for *ventral*) as representatives of the three classes of motor neurons because these ventral muscle-innervating neurons could be easily identified based on their anatomical locations (Figure 1A). We first examined the effect of *slo-2* mutation on delayed outward current in response to voltage steps (−60 to +70 mV at 10-mV intervals). The amplitude of delayed outward current was greatly decreased in *slo-2(nf101)*, a putative null resulting from a deletion³⁰, compared with wild type in all the motor neurons (Figure 1B). The decrease was more severe in VA5 and VB6 than VD5. Compared with wild type, delayed outward current at +70 mV decreased by 80% in VA5 (168.9 ± 16.6 versus 33.6 ± 2.4 pA/pF), 67% in VB6 (176.1 ± 13.4 versus 58.1 ± 3.1 pA/pF), and 33% in VD5 (197.1 ± 12.5 versus 131.9 ± 5.6 pA/pF) (Figure 1B). The deficiency of delayed outward current in the mutant was rescued by expressing a SLO-2::GFP fusion protein, in which GFP coding sequence was fused in-frame to the 3'-end of *slo-2b* (F08B12.3b) cDNA (www.wormbase.org)²³, under the control of the pan-neuronal *rab-3* promoter (*Prab-3*)^{31, 32} (Figure 1B), suggesting that the deficiency resulted from *slo-2* mutation in neurons, and that the SLO-2::GFP fusion protein was functional.

The persistence of some delayed outward current in *slo-2(nf101)* suggests that there is at least one more K⁺ channel functioning in motor neurons. It is difficult to do a comprehensive survey for the many voltage-gated K⁺ channels existing in *C. elegans*³³. Previous studies show that three voltage-gated K⁺ channels are important to outward current in *C. elegans* body-wall muscle cells, including SLO-2, SHK-1 (*Shaker* or K_V1) and SHL-1 (*Shal* or K_V4), with SLO-2 and SHK-1 conducting delayed outward current and SHL-1 conducting a fast and transient outward current^{25, 34, 35}. This knowledge was used as a guide in identifying the remaining K⁺ channel(s) contributing to outward current in motor neurons. SLO-1, the *C. elegans* Slo1/BK channel, was also included in our analyses because it is expressed in *C. elegans* motor neurons and plays an important role in regulating neurotransmitter release³⁶. The mutants analyzed included *shk-1(ok1581)*, *shl-1(ok1168)* and *slo-1(md1745)*, which are all putative nulls^{25, 35, 36}. Delayed outward current was normal in VA5 and VB6 of all the mutants (Figure 1B) but greatly decreased in VD5 of *shk-1(ok1581)* (Figure 1B). In fact, delayed outward current of VD5 was decreased to a larger degree in *shk-1(ok1581)* (45%) than *slo-2(nf101)* (33%) at +70 mV (wild type 197.1 ± 12.5 pA/pF; *shk-1* 108.9 ± 15.6 pA/pF; *slo-2* 131.9 ± 5.6 pA/pF) and was essentially absent in the double mutant (Figure 1B).

Collectively, the aforementioned observations suggest that delayed outward current of VA5 and VB6 results primarily from SLO-2 with a small contribution from an unidentified channel(s), whereas that of VD5 results almost completely from SHK-1 and SLO-2.

SLO-2 regulates membrane potential of motor neurons

In wild-type worms, the resting membrane potential was −71.7 ± 2.4 mV in VA5, −53.2 ± 2.5 mV in VB6 and −45.8 ± 1.9 mV in VD5. It became significantly less hyperpolarized in *slo-2(nf101)* but was restored to wild-type level in the *slo-2(nf101)* strain expressing *Prab-3::SLO-2::GFP* (Table 1). In contrast, mutants of the other K⁺ channels did not show a change of the resting membrane potential compared with wild type (Table 1). These

observations suggest that SLO-2 plays an important role in setting the resting membrane potential of both cholinergic and GABAergic motor neurons.

To assess the role of SLO-2 in regulating motor neuron activity, we analyzed spontaneous membrane voltage changes of VA5. In both wild type and *slo-2(nf101)*, the membrane voltage alternated between the resting membrane potential and an up-state, with apparent spontaneous postsynaptic potentials decorating both periods (Figure 2A). The up-state often reached a similar level in each recording, and never overshoot (Figure 2A). Compared with wild type, the up-state of *slo-2(nf101)* was 61% smaller in amplitude (33.4 ± 1.4 versus 13.1 ± 0.9 mV) and 45% longer in duration (14.9 ± 1.5 versus 21.6 ± 2.6 sec) without a change in frequency (Figure 2B). Since up-state potential (the mean membrane potential during the upstate) was similar between wild type and *slo-2(nf101)* (Figure 2B), the smaller up-state amplitude of the mutant resulted from the elevated resting membrane potential.

SLO-2 regulates neurotransmitter release

To determine whether SLO-2 in motor neurons regulates synaptic transmission, we analyzed spontaneous and evoked PSCs at the *C. elegans* neuromuscular junction. We first focused on spontaneous PSC bursts, defined as an apparent increase in PSC frequency with a persistent current lasting >3 sec, because they are the physiological signals used by motor neurons to control muscle contractility²⁷. The persistent current, appearing as an apparent downward shift of the baseline, was used to demarcate PSC bursts, as described previously²⁷. Cholinergic PSC bursts were isolated by using pipette and extracellular solutions with the Cl⁻ equilibrium potential equal to the holding potential (-60 mV). Compared with wild type, *slo-2(nf101)* showed significantly longer duration and higher charge transfer rate in PSC bursts, which were restored to wild-type level when SLO-2::GFP was expressed in neurons (Figure 3A, B). The main cause for the higher charge transfer rate of PSC bursts in *slo-2(nf101)* was a larger persistent current because amplitude of the persistent current increased by 87% (wild type 4.6 ± 0.5 pA; *slo-2* 8.6 ± 0.8 pA) (Figure 3B) but frequency and amplitude of intra-burst PSC events were unaltered compared with wild type (Figure 3C).

The larger persistent current of cholinergic PSC bursts observed in *slo-2(nf101)* could have resulted from either increased neurotransmitter release or increased postsynaptic receptor sensitivity to ACh. To examine the second possibility, we compared the amplitude of inward current caused by pressure-ejecting exogenous ACh (100 μ M) to body-wall muscle cells between wild type and *slo-2(nf101)*. A similar experiment with exogenous GABA (100 μ M) was also performed although GABA did not contribute to the PSC bursts under the experimental conditions²⁷. We found that amplitudes of ACh- and GABA-induced inward current were similar between wild type and *slo-2(nf101)* (Figure 4A). Thus, the larger persistent current of PSC bursts in *slo-2(nf101)* did not result from an increased postsynaptic receptor function or expression.

We also compared evoked PSCs caused by electric stimulation of motor neurons between wild type and *slo-2(nf101)*. Evoked PSCs were analyzed in the presence of two different $[Ca^{2+}]_o$ (5 mM and 0.5 mM) because an effect of *slo-2* mutation on the evoked responses could potentially vary depending on $[Ca^{2+}]_o$, as is the case with *slo-1* mutation³⁷. We found

that evoked PSCs were similar in amplitude between wild type and *slo-2(lf)* in the presence of either 5 mM or 0.5 mM $[Ca^{2+}]_o$ (Figure 4B), suggesting that SLO-2 does not regulate neurotransmitter release caused by strong non-physiological stimuli.

SLO-2 in motor neurons requires Cl^- and Ca^{2+} for activation

Analyses with inside-out patches from *Xenopus* oocytes show that SLO-2 has a mean single channel conductance of 110 pS in symmetrical K^+ , and is activated synergistically by Ca^{2+} and Cl^- on the intracellular side²³. However, single-channel conductance of SLO-2 in neurons has not been reported, the concentration of free Ca^{2+} required for significant SLO-2 activity²³ is much higher than what could possibly be reached in the bulk cytoplasm under physiological conditions, and the reported Cl^- sensitivity of SLO-2 was rebutted by a recent study³⁸. We therefore performed experiments to assess the single-channel conductance of SLO-2 in motor neurons and to determine whether SLO-2 in motor neurons is sensitive to Ca^{2+} and Cl^- . First, we recorded SLO-2 single channel activities in inside-out patches held at a series of voltages in the presence of symmetrical K^+ solutions to determine SLO-2 single channel conductance. In wild type, each patch typically showed activities of a few channels, which were apparently of the same type (Figure 5A). In contrast, similar single-channel opening events were never observed in *slo-2(lf)* (Figure 5A). We determined SLO-2 single channel conductance from the slope of a linear fit to SLO-2 single channel current amplitudes at the various voltages, and found it to be 117 ± 2 pS in VA5, 120 ± 2 pS in VB6 and 111 ± 2 pS in VD5 (Figure 5B). These values are similar to those of SLO-2 expressed in *Xenopus* oocytes²³ and in cultured body-wall muscle cells³⁴. Next, we analyzed the effect of intracellular Cl^- on SLO-2 by reducing $[Cl^-]$ from 128.5 mM to 15.3 mM in the standard pipette solution. This treatment essentially abolished SLO-2 current in wild-type worms, as suggested by the similar outward current between WT with low $[Cl^-]_i$ and *slo-2(lf)* with high $[Cl^-]_i$, and the lack of an effect of the low $[Cl^-]_i$ on outward current in *slo-2(lf)* (Figure 6A). Finally, we analyzed SLO-2 Ca^{2+} dependence. In recording the whole-cell current, the concentration of free Ca^{2+} in the pipette solution was ~ 50 nM, which was not expected to cause significant SLO-2 activation²³. We hypothesized that extracellular Ca^{2+} plays a role in SLO-2 activation by establishing Ca^{2+} microdomains at the inner openings of Ca^{2+} permeable channels, as is the case for mammalian Slo2 activation by extracellular $Na^{+4, 5}$. We therefore examined the effects of varying $[Ca^{2+}]_o$ between 5 mM and zero on SLO-2 single channel activity in outside-out patches with little free Ca^{2+} (~ 50 nM) in the pipette solution. Indeed, SLO-2 activity was high when $[Ca^{2+}]_o$ was 5 mM but greatly decreased after $[Ca^{2+}]_o$ was changed to zero (Figure 6B). Taken together, our observations suggest that SLO-2 in motor neurons depends on both Cl^- and Ca^{2+} for activation, and that extracellular Ca^{2+} plays an important role in SLO-2 activation.

Ca^{2+} entry through EGL-19 is important to SLO-2 activation

Given that SLO-2 was activated by Ca^{2+} entering the cell, there must be a Ca^{2+} channel(s) mediating the Ca^{2+} entry. We first examined potential contributions by VGCCs. The *C. elegans* genome contains three genes encoding the pore-forming α_1 -subunit of VGCCs, including *egl-19* (Ca_v1/L -type), *unc-2* ($Ca_v2/N, P, Q$ -type), and *cca-1* (Ca_v3/T -type)³⁹. We selected mutants of these genes for analyses. For *unc-2* and *cca-1*, we analyzed the severe *lf* or null mutants *unc-2(e55)* and *cca-1(ad1650)*^{40, 41}. For *egl-19*, we analyzed the gain-of-

function mutant *egl-19(ad695)* and the hypomorphic mutant *egl-19(n582)* because null mutants die at embryonic stages⁴². Compared with wild type, *egl-19(ad695)* caused a significantly larger delayed outward current in all the motor neurons (VA5, VB6 and VD5) whereas *egl-19(n582)* showed an opposite effect in VA5 and VB6 (Figure 7). These effects of the *egl-19* mutants were not observed in the presence of *slo-2(nf101)* (Figure 7), suggesting that EGL-19 regulates delayed outward current through SLO-2. The insignificant effect of *egl-19(n582)* on delayed outward current in VD5 (Figure 7) could be due to the relatively small SLO-2 current in VD5 (Figure 1).

Delayed outward current was similar between wild type and either *unc-2(e55)* or *cca-1(ad1650)* (Figure 8), suggesting that UNC-2 and CCA-1 do not play a role in SLO-2 activation. In addition to the VGCCs, we assessed potential contributions by several other proteins implicated in either Ca²⁺ entry or Ca²⁺ release from endoplasmic reticulum, including TRP-1 (canonical transient receptor potential channel, TRPC)⁴³, CLHM-1 (calcium homeostasis modulator, Calhm)⁴⁴, NCA-1 and NCA-2 (putative cation channels)^{45, 46}, and UNC-68 (ryanodine receptor)^{47, 48} by analyzing whole-cell current in corresponding mutants. The mutant strains used included *trp-1(ok323)*^{49, 50}, *clhm-1(ok3617)*⁴⁴, *unc-68(r1162)*⁴⁷ and the double mutant *nca-1(gk9);nca-2(gk5)*^{45, 46, 51}, which are either nulls or severe *lf* mutants. Delayed outward current was normal in all these mutants (Figure 8). Taken together, the aforementioned observations suggest that EGL-19 is likely the primary, if not the only, Ca²⁺ channel mediating SLO-2 activation in motor neurons.

Discussion

Our electrophysiological data indicate that SLO-2 is the primary contributor to delayed outward current in A and B class motor neurons, and one of two major contributors to this current in D class motor neurons. These observations are reminiscent of those with rat central neurons where Slo2 channels contribute to a large portion of delayed outward current⁴⁻⁶. The similar observations with rat and *C. elegans* suggest that these channels began to assume the important task of conducting delayed outward current early in evolution, and that their existence has been indispensable.

The resting membrane potential of mammalian neurons is generally close to the K⁺ equilibrium potential due to the function of background K⁺ channels. Two-pore domain K⁺ (K2P) channels appear to be important molecular entities of the background K⁺ channels because they are largely voltage-independent⁵². The *C. elegans* genome has 46 K2P genes³³. Although no experimental evidence is currently available, it is conceivable that some of these channels may play roles in setting the resting membrane potential. The present study shows that SLO-2, which is not a K2P channel, plays an important role in setting the resting membrane potential of motor neurons. A similar role of SLO-2 has been observed in *C. elegans* body-wall muscle²⁵. Thus, SLO-2 might be important in setting the resting membrane potential of many *C. elegans* neurons and muscle cells.

slo-2 mutation resulted in a longer duration and a larger persistent current of PSC bursts compared with wild type, suggesting that a physiological function of SLO-2 is to shorten the

duration and decrease the charge transfer rate of PSC bursts. SLO-2 likely performs these physiological functions by regulating neurotransmitter release because body-wall muscle sensitivities to neurotransmitters are normal in *slo-2* mutant. Given that PSC bursts are the physiological signals used by motor neurons to control body-wall muscle cells²⁷, SLO-2 likely plays an important role in regulating muscle function. This physiological function of SLO-2 could be related to its effect on the resting membrane potential of motor neurons and its interactions with other proteins such as EGL-19.

The substantial decrease of SLO-2 single channel activity in outside-out patches following the removal of Ca^{2+} on the extracellular side suggests that SLO-2 activity depends on Ca^{2+} entry. EGL-19 appeared to play an important role in SLO-2 activation as SLO-2 current was significantly increased in *egl-19(gf)* but decreased in *egl-19(hypomorph)*. Indeed, EGL-19 might be the only channel with this function given that mutants of a variety of other genes known to be important to either entry of extracellular Ca^{2+} or release of Ca^{2+} from the endoplasmic reticulum did not show a change of SLO-2 current. The coupling of SLO-2 activation to Ca^{2+} entry through EGL-19 explains why large SLO-2 current is observed in *C. elegans* motor neurons in whole-cell voltage-clamp experiments with very low free Ca^{2+} in the pipette solution. The dependence of SLO-2 activity on EGL-19 is analogous to that of mammalian Slo2 on tetrodotoxin-sensitive Na^+ channels^{4,5}. *C. elegans* does not have any genes encoding voltage-gated Na^+ channels and likely uses Ca^{2+} exclusively for carrying excitatory inward current³⁹, which is in contrast to mammals in which Na^+ action potentials generally underlie cellular excitability. It thus appears that coupling channel activation to the entry of a cation is a conserved property of SLO-2/Slo2 channels but evolution has tuned this property to match the dominant ion used in cellular excitation in each species.

The *C. elegans* Slo family of K^+ channels includes two members: SLO-1 and SLO-2^{24, 33}. *slo-1(lf)* also prolongs the duration of PSC bursts²⁷. However, there are major differences in synaptic phenotypes between *slo-1* and *slo-2* mutants. Unlike *slo-2(lf)*, *slo-1(lf)* does not alter the persistent current of PSC bursts but may cause larger evoked PSC amplitude at the *C. elegans* neuromuscular junction compared with wild type^{27, 37, 53}. Thus, SLO-1 and SLO-2 likely inhibit neurotransmitter release through somewhat different mechanisms, which could be related to their different subcellular localization and/or functional coupling to different voltage-gated Ca^{2+} channels. While SLO-1 is localized at the presynaptic site⁵³ and likely regulated by Ca^{2+} entry through UNC-2, which is also localized at the presynaptic site⁵⁴, SLO-2 might be localized to other subcellular domains and coupled to Ca^{2+} entry through EGL-19.

SLO-1 did not show a detectable contribution to the whole-cell current of motor neurons in spite of its important role in regulating neurotransmitter release. There are two possible causes for this discrepancy. First, the free $[\text{Ca}^{2+}]$ of the recording pipette (~50 nM) was insufficient to allow significant SLO-1 activation. Second, SLO-1 current at presynaptic sites, which could potentially result from a coupling to Ca^{2+} entry through UNC-2, might have been shunted before reaching the soma. We have noted a similar discrepancy between SLO-1 function and its contribution to whole-cell current in *C. elegans* body-wall muscle, where SLO-1 is expressed³⁶ and plays an important role in regulating Ca^{2+} transients⁵³ but whole-cell current was indistinguishable between wild type and *slo-1* null mutant even when

a pipette solution containing 20 μM free Ca^{2+} concentration was used in the recording (unpublished).

slo-2 mutant worms displayed no obvious locomotion defects, which is somewhat surprising given that SLO-2 is an important K^+ channel in both body-wall muscle cells^{15, 25, 34} and motor neurons. This is analogous to the movement phenotypes of *slo-1* mutants. Although SLO-1 also plays important physiological roles in both neurons^{36, 55} and body-wall muscle cells^{56–58}, *slo-1* mutants only show a slightly larger head bending angle compared with wild type, which results from SLO-1 deficiency in body-wall muscle cells, and may be detected only by either a trained observer or computer-based analyses^{59, 60}. Perhaps potential effects of SLO-2 deficiency on behavioral phenotypes would become more obvious in a sensitized genetic background or under some specific conditions such as hypoxia¹⁵.

The original paper on SLO-2 reported that SLO-2 heterologously expressed in *Xenopus* oocytes is activated by Cl^- on the intracellular side²³. Consistently, the concentration of Cl^- in the recording pipette solution was found to have a large effect on SLO-2 activity of *C. elegans* body-wall muscle cells *in situ*³⁴. However, the Cl^- dependence of SLO-2 was challenged by a recent study, which showed that at least two isoforms of SLO-2, including the original one used in the heterologous expression experiments, are Cl^- -insensitive³⁸. It was suggested that the apparent Cl^- dependence of SLO-2 observed in the earlier study reflected contamination by an endogenous Cl^- current present in *Xenopus* oocytes³⁸. Our observations provide evidence that SLO-2 in native motor neurons is a Cl^- -sensitive channel.

Both the human genome and *C. elegans* genome contain over 70 potassium channel genes^{33, 61}. The fact that SLO-2/Slo2 channels play a major role in conducting delayed outward current in neurons of both species suggests that this subfamily of K^+ channels likely performs conserved physiological functions of unusual importance. It will be interesting to know whether mammalian Slo2 channels also control the resting membrane potential and regulate synaptic transmission, and how their physiological functions are modulated *in vivo*. Since knockout mice of both Slo2 genes (KCNT1 and KCNT2) are now available from the Jackson lab (MGI:1924627 and 3036273), it is desirable to compare between wild type and the knockout mice the resting membrane potential and post-synaptic currents in selected central neurons. In addition, many Slo2 mutations identified in human epileptic patients may be introduced into worm SLO-2 to investigate how these mutations affect channel function and/or expression *in vivo*. In some cases, expression of a mutated channel may cause an obvious behavioral phenotype, which could serve as a very useful tool for identifying conserved Slo2 channel regulatory proteins through mutant screen in this genetically tractable model organism.

Methods

C. elegans culture and strains

C. elegans hermaphrodites were raised on nematode growth medium plates spotted with a layer of OP50 *Escherichia coli* at 21°C inside an environmental chamber. The strains used included wild type (Bristol N2), *slo-2(nf101)*, *shk-1(ok1581)*, *shl-1(ok1168)*, *slo-1(md1745)*,

egl-19(ad695), *egl-19(n582)*, *unc-2(e55)*, *cca-1(ad1650)*, *nca-1(gk9);nca-2(gk5)*,
trp-1(ok323), *clhm-1(ok3617)*, *unc-68(r1162)*, *slo-2(nf101);shk-1(ok1581)*,
slo-2(nf101);egl-19(ad695), and *slo-2(nf101);egl-19(n582)*.

Mutant Rescue

Neuron-specific rescue was performed by injecting a plasmid containing the pan-neuronal *Prab-3* and full-length *slo-2b* cDNA (F08B12.3b) (www.wormbase.org)²³ fused in-frame at its 3'-end to GFP coding sequence into *slo-2(nf101)* using a standard technique⁶².

Electrophysiology

All electrophysiological experiments were performed with adult hermaphrodites. An animal was immobilized on a glass coverslip by applying VetbondTM Tissue Adhesive (3M Company, St. Paul, MN). Application of the glue was generally restricted to the dorsal anterior portion (excluding the head) of the animal, allowing the head and tail to sway freely during the experiment. A short (~300 μ m) longitudinal incision was made along the glued region. After clearing the viscera by suction through a glass pipette, the cuticle flap was folded back and glued to the coverslip, exposing several ventral body-wall muscle cells and a small number of motor neurons anterior to the vulva. Borosilicate glass pipettes were used as electrodes for recording whole-cell and single-channel currents. Pipette tip resistance for recording muscle cell current was 3–5 M Ω whereas that for recording motor neuron current was ~20 M Ω . The dissected worm preparation was treated briefly with collagenase A (Roche Applied Science, catalogue number 10103578001, 0.5 mg/ml for 10–15 sec) and perfused with the extracellular solution for 5 to 10-fold of bath volume. Classical whole-cell configuration was obtained by applying a negative pressure to the recording pipette. Inside-out patches were obtained by quickly pulling away the recording pipette after the formation of a gigaohm seal whereas outside-out patches were obtained by slowly pulling away the recording pipette after achieving the whole-cell configuration. Current- and voltage-clamp experiments were performed with a Multiclamp 700B amplifier (Molecular Devices, Sunnyvale, CA, USA) and the Clampex software (version 10, Molecular Devices). Data were sampled at a rate of 10 kHz after filtering at 2 kHz. Spontaneous membrane potential changes were recorded using the current-clamp technique without current injection. Motor neuron whole-cell outward currents were recorded by applying a series of voltage steps (–60 to +70 mV at 10-mV intervals, 1200 ms pulse duration) from a holding potential of –60 mV. Evoked PSC, spontaneous PSC, and exogenous ACh- or GABA-induced PSC were recorded from body-wall muscle cells at a holding potential of –60 mV. Evoked PSC was caused by applying an electric stimulus at a saturating strength (20 V, 0.5 ms) through a glass pipette electrode placed near the ventral nerve cord. The stimulus was generated by a square pulse stimulator (S48, Grass Technologies, Warwick, RI, USA). To obtain representative evoked PSC from each preparation, the position of the electrode was adjusted until a maximal evoked PSC peak amplitude was observed. Muscle responses to exogenous ACh and GABA were caused by puffing the chemicals (100 μ M) through a glass pipette using a FemtoJet injector (Eppendorf) with the pressure pulse set at 0.2 psi and 0.1 s.

Solutions

Three different extracellular solutions and three different pipette solutions were used, as specified in figure legends. Extracellular solution I contained (in mM) 140 NaCl, 5 KCl, 5 CaCl₂, 5 MgCl₂, 11 dextrose and 5 HEPES (pH 7.2). Extracellular solution II differed from extracellular solution I in that CaCl₂ was reduced to 0.5 mM. Extracellular solution III differed from extracellular solution I in that CaCl₂ was eliminated, 5 mM EGTA was added, and NaCl was increased to 150 mM. Pipette solution I contained (in mM) 120 KCl, 20 KOH, 5 Tris, 0.25 CaCl₂, 4 MgCl₂, 36 sucrose, 5 EGTA, and 4 Na₂ATP (pH 7.2). Pipette solution II differed from pipette solution I in that 113.2 KCl was substituted by K⁺ gluconate. Pipette solution III contained (in mM) 150 K⁺ gluconate, 1 Mg²⁺ gluconate, and 10 HEPES (pH 7.2). The bath solution used in inside-out patch experiments contained (in mM) 100 K⁺ gluconate, 50 KCl, 1 Mg²⁺ gluconate, 0.1 Ca²⁺ gluconate and 10 HEPES (pH 7.2).

Data Analyses

Amplitudes of whole-cell current in response to voltage steps were determined from the mean current during the last 100 ms of the 1200-ms voltage pulses using the Clampfit software (version 10, Molecular Devices). SPSS software (IBM corp., New York) was used for comparing the current among different genotypes by two-way mixed model analyses of variance (*ANOVA*). In these analyses, voltage steps were treated as within-subject variables whereas genotypes as between-subject variables. Tukey's post hoc tests were used to determine whether a statistically significant difference exists between specified genotypes. All genotypes shown in Figures 1, 6, 7 and 8 were analyzed together so that valid statistical comparisons could be made among them.

SLO-2 single channel amplitude and open probability were quantified using Clampfit. PSC bursts were identified as an apparent increase in PSC frequency with a persistent current lasting > 3 sec²⁷. The duration, mean persistent current amplitude, and mean charge transfer rate of PSC bursts were determined with Clampfit. The frequency and amplitude of spontaneous PSCs were quantified using MiniAnalysis (Synaptosoft, Inc., Decatur, GA) with the detection threshold set at 10 pA for initial automatic event detection, followed by visual inspections to include missed events (< 5 pA) and to exclude false events resulting from baseline fluctuations. The software was set to search for a baseline 3 ms before a PSC event and use the average of a 1-ms period as the baseline level. Peak amplitudes of evoked PSCs and of muscle responses to exogenous ACh or GABA were quantified using Clampfit. The average of the largest two evoked PSCs recorded from each muscle cell was used for statistical comparisons. Up-state was defined as a sudden increase (> 5 mV) in the membrane potential lasting longer than 3 sec. Up-state potential was the mean membrane voltage during the up-state (quantified with Clampfit) whereas up-state amplitude was the voltage difference between up-state potential and the resting membrane potential. All the up-states of each recording (3 to 5 min) were analyzed to obtain an averaged value of each parameter (*e. g.* amplitude, duration) before statistical analyses. Statistical comparisons were performed with OriginPro (version 9, OriginLab, Northampton, MA, USA) using either one-way *ANOVA* or unpaired *t*-test (depending on whether there were more than two groups). All values are shown as mean ± S.E. *p* < 0.05 is considered to be statistically significant.

The sample size (n) equals the number of cells or membrane patches analyzed. Data graphing was performed with OriginPro.

Acknowledgments

This work was supported by National Institute of Health (1R01MH085927, ZWW). The authors wish to thank Caenorhabditis Genetics Center (USA), Erik Jorgensen lab, and Lawrence Salkoff lab for mutant strains.

References

1. Trussell, LO.; Roberts, MT. The role of potassium channels in the regulation of neurotransmitter release. In: Wang, ZW., editor. *Molecular Mechanisms of Neurotransmitter Release*. Humana Press; 2008.
2. Bhattacharjee A, Gan L, Kaczmarek LK. Localization of the Slack potassium channel in the rat central nervous system. *J Comp Neurol*. 2002; 454:241–254. [PubMed: 12442315]
3. Bhattacharjee A, von Hehn CA, Mei X, Kaczmarek LK. Localization of the Na⁺-activated K⁺ channel Slick in the rat central nervous system. *J Comp Neurol*. 2005; 484:80–92. [PubMed: 15717307]
4. Hage TA, Salkoff L. Sodium-activated potassium channels are functionally coupled to persistent sodium currents. *J Neurosci*. 2012; 32:2714–2721. [PubMed: 22357855]
5. Budelli G, et al. Na⁺-activated K⁺ channels express a large delayed outward current in neurons during normal physiology. *Nat Neurosci*. 2009; 12:745–750. [PubMed: 19412167]
6. Lu S, Das P, Fadool DA, Kaczmarek LK. The slack sodium-activated potassium channel provides a major outward current in olfactory neurons of Kv1.3^{-/-} super-smeller mice. *J Neurophysiol*. 2010; 103:3311–3319. [PubMed: 20393063]
7. Huang F, et al. TMEM16C facilitates Na⁺-activated K⁺ currents in rat sensory neurons and regulates pain processing. *Nat Neurosci*. 2013; 16:1284–1290. [PubMed: 23872594]
8. Nuwer MO, Picchione KE, Bhattacharjee A. PKA-induced internalization of slack KNa channels produces dorsal root ganglion neuron hyperexcitability. *J Neurosci*. 2010; 30:14165–14172. [PubMed: 20962237]
9. Zhang Y, et al. Regulation of neuronal excitability by interaction of fragile x mental retardation protein with slack potassium channels. *J Neurosci*. 2012; 32:15318–15327. [PubMed: 23115170]
10. Barcia G, et al. *De novo* gain-of-function *KCNT1* channel mutations cause malignant migrating partial seizures of infancy. *Nat Genet*. 2012; 44:1255–1259. [PubMed: 23086397]
11. Heron SE, et al. Missense mutations in the sodium-gated potassium channel gene *KCNT1* cause severe autosomal dominant nocturnal frontal lobe epilepsy. *Nat Genet*. 2012; 44:1188–1190. [PubMed: 23086396]
12. Vanderver A, et al. Identification of a novel *de novo* p.Phe932Ile *KCNT1* mutation in a patient with leukoencephalopathy and severe epilepsy. *Pediatr Neurol*. 2013
13. Ishii A, et al. A recurrent *KCNT1* mutation in two sporadic cases with malignant migrating partial seizures in infancy. *Gene*. 2013; 531:467–471. [PubMed: 24029078]
14. Dhamija R, Wirrell E, Falcao G, Kirmani S, Wong-Kisiel LC. Novel *de novo* *SCN2A* mutation in a child with migrating focal seizures of infancy. *Pediatr Neurol*. 2013
15. Yuan A, et al. The sodium-activated potassium channel is encoded by a member of the *Slo* gene family. *Neuron*. 2003; 37:765–773. [PubMed: 12628167]
16. Bhattacharjee A, et al. Slick (Slo2.1), a rapidly-gating sodium-activated potassium channel inhibited by ATP. *J Neurosci*. 2003; 23:11681–11691. [PubMed: 14684870]
17. Dryer SE. Molecular identification of the Na⁺-activated K⁺ channel. *Neuron*. 2003; 37:727–728. [PubMed: 12628162]
18. Kaczmarek LK. Slack, Slick and Sodium-Activated Potassium Channels. *ISRN Neurosci*. 2013
19. Bhattacharjee A, Kaczmarek LK. For K⁺ channels, Na⁺ is the new Ca²⁺ Trends Neurosci. 2005; 28:422–428. [PubMed: 15979166]

20. Wallen P, et al. Sodium-dependent potassium channels of a Slack-like subtype contribute to the slow afterhyperpolarization in lamprey spinal neurons. *J Physiol*. 2007; 585:75–90. [PubMed: 17884929]
21. Yang B, Desai R, Kaczmarek LK. Slack and Slick K(Na) channels regulate the accuracy of timing of auditory neurons. *J Neurosci*. 2007; 27:2617–2627. [PubMed: 17344399]
22. Nanou E, et al. Na⁺-mediated coupling between AMPA receptors and K_{Na} channels shapes synaptic transmission. *PNAS*. 2008; 105:20941–20946. [PubMed: 19095801]
23. Yuan A, et al. SLO-2, a K⁺ channel with an unusual Cl⁻ dependence. *Nat Neurosci*. 2000; 3:771–779. [PubMed: 10903569]
24. Salkoff L, Butler A, Ferreira G, Santi C, Wei A. High-conductance potassium channels of the SLO family. *Nat Rev Neurosci*. 2006; 7:921–931. [PubMed: 17115074]
25. Liu P, et al. Genetic dissection of ion currents underlying all-or-none action potentials in *C. elegans* body-wall muscle cells. *J Physiol*. 2011; 589:101–117. [PubMed: 21059759]
26. Lim HH, et al. Identification and characterization of a putative *C. elegans* potassium channel gene (*Ce-slo-2*) distantly related to Ca²⁺-activated K⁺ channels. *Gene*. 1999; 240:35–43. [PubMed: 10564810]
27. Liu P, Chen B, Wang ZW. Postsynaptic current bursts instruct action potential firing at a graded synapse. *Nat Commun*. 2013; 4:1911. [PubMed: 23715270]
28. de Bono M, Maricq AV. Neuronal substrates of complex behaviors in *C. elegans*. *Annu Rev Neurosci*. 2005; 28:451–501. [PubMed: 16022603]
29. Chalfie, M.; White, J. Researchers TCoCe. The nervous system. In: Wood, WB., editor. *The Nematode Caenorhabditis elegans*. Cold Spring Harbor Laboratory Press; 1988.
30. Wei A, et al. Efficient isolation of targeted *Caenorhabditis elegans* deletion strains using highly thermostable restriction endonucleases and PCR. *Nucleic Acids Res*. 2002; 30:e110. [PubMed: 12384612]
31. Mahoney TR, et al. Regulation of Synaptic Transmission by RAB-3 and RAB-27 in *Caenorhabditis elegans*. *Mol Biol Cell*. 2006; 17:2617–2625. [PubMed: 16571673]
32. Nonet ML, et al. *Caenorhabditis elegans* rab-3 mutant synapses exhibit impaired function and are partially depleted of vesicles. *The Journal of neuroscience: the official journal of the Society for Neuroscience*. 1997; 17:8061–8073. [PubMed: 9334382]
33. Salkoff, L., et al. *WormBook*. The *C. elegans* Research Community. *WormBook*; 2005. Potassium channels in *C. elegans*. <http://www.wormbook.org>
34. Santi CM, et al. Dissection of K⁺ currents in *Caenorhabditis elegans* muscle cells by genetics and RNA interference. *Proc Natl Acad Sci U S A*. 2003; 100:14391–14396. [PubMed: 14612577]
35. Fawcett GL, et al. Mutant analysis of the Shal (Kv4) voltage-gated fast transient K⁺ channel in *Caenorhabditis elegans*. *J Biol Chem*. 2006; 281:30725–30735. [PubMed: 16899454]
36. Wang ZW, Saifee O, Nonet ML, Salkoff L. SLO-1 potassium channels control quantal content of neurotransmitter release at the *C. elegans* neuromuscular junction. *Neuron*. 2001; 32:867–881. [PubMed: 11738032]
37. Liu Q, Chen B, Ge Q, Wang ZW. Presynaptic Ca²⁺/calmodulin-dependent protein kinase II modulates neurotransmitter release by activating BK channels at *Caenorhabditis elegans* neuromuscular junction. *J Neurosci*. 2007; 27:10404–10413. [PubMed: 17898212]
38. Zhang Z, et al. SLO-2 isoforms with unique Ca²⁺- and voltage-dependence characteristics confer sensitivity to hypoxia in *C. elegans*. *Channels (Austin)*. 2013; 7
39. Bargmann CI. Neurobiology of the *Caenorhabditis elegans* genome. *Science*. 1998; 282:2028–2033. [PubMed: 9851919]
40. Bauer Huang SL, et al. Left-right olfactory asymmetry results from antagonistic functions of voltage-activated calcium channels and the Raw repeat protein OLRN-1 in *C. elegans*. *Neural Dev*. 2007; 2:24. [PubMed: 17986337]
41. Steger KA, Shtonda BB, Thacker C, Snutch TP, Avery L. The *C. elegans* T-type calcium channel CCA-1 boosts neuromuscular transmission. *J Exp Biol*. 2005; 208:2191–2203. [PubMed: 15914662]

42. Lee RY, Lobel L, Hengartner M, Horvitz HR, Avery L. Mutations in the $\alpha 1$ subunit of an L-type voltage-activated Ca^{2+} channel cause myotonia in *Caenorhabditis elegans*. *EMBO J*. 1997; 16:6066–6076. [PubMed: 9321386]
43. Feng Z, et al. A *C. elegans* model of nicotine-dependent behavior: regulation by TRP-family channels. *Cell*. 2006; 127:621–633. [PubMed: 17081982]
44. Tanis JE, et al. CLHM-1 is a functionally conserved and conditionally toxic Ca^{2+} -permeable ion channel in *Caenorhabditis elegans*. *J Neurosci*. 2013; 33:12275–12286. [PubMed: 23884934]
45. Yeh E, et al. A putative cation channel, NCA-1, and a novel protein, UNC-80, transmit neuronal activity in *C. elegans*. *PLoS Biol*. 2008; 6:e55. [PubMed: 18336069]
46. Jospin M, et al. UNC-80 and the NCA ion channels contribute to endocytosis defects in synaptotagmin mutants. *Curr Biol*. 2007; 17:1595–1600. [PubMed: 17825559]
47. Maryon EB, Coronado R, Anderson P. *unc-68* encodes a ryanodine receptor involved in regulating *C. elegans* body-wall muscle contraction. *J Cell Biol*. 1996; 134:885–893. [PubMed: 8769414]
48. Liu Q, et al. Presynaptic ryanodine receptors are required for normal quantal size at the *Caenorhabditis elegans* neuromuscular junction. *J Neurosci*. 2005; 25:6745–6754. [PubMed: 16033884]
49. Hyde R, Corkins ME, Somers GA, Hart AC. PKC-1 acts with the ERK MAPK signaling pathway to regulate *Caenorhabditis elegans* mechanosensory response. *Genes Brain Behav*. 2011; 10:286–298. [PubMed: 21143768]
50. Glauser DA, et al. Heat avoidance is regulated by transient receptor potential (TRP) channels and a neuropeptide signaling pathway in *Caenorhabditis elegans*. *Genetics*. 2011; 188:91–103. [PubMed: 21368276]
51. Humphrey JA, et al. A putative cation channel and its novel regulator: cross-species conservation of effects on general anesthesia. *Current biology: CB*. 2007; 17:624–629. [PubMed: 17350263]
52. Enyedi P, Czirjak G. Molecular background of leak K^{+} currents: two-pore domain potassium channels. *Physiol Rev*. 2010; 90:559–605. [PubMed: 20393194]
53. Chen B, Liu P, Zhan H, Wang ZW. Dystrobrevin Controls Neurotransmitter Release and Muscle Ca^{2+} Transients by Localizing BK Channels in *Caenorhabditis elegans*. *J Neurosci*. 2011; 31:17338–17347. [PubMed: 22131396]
54. Saheki Y, Bargmann CI. Presynaptic $\text{CaV}2$ calcium channel traffic requires CALF-1 and the $\alpha 2\delta$ subunit UNC-36. *Nat Neurosci*. 2009; 12:1257–1265. [PubMed: 19718034]
55. Davies AG, et al. A central role of the BK potassium channel in behavioral responses to ethanol in *C. elegans*. *Cell*. 2003; 115:655–666. [PubMed: 14675531]
56. Chen B, et al. A novel auxiliary subunit critical to BK channel function in *Caenorhabditis elegans*. *J Neurosci*. 2010; 30:16651–16661. [PubMed: 21148004]
57. Kim H, et al. The dystrophin complex controls bk channel localization and muscle activity in *Caenorhabditis elegans*. *PLoS Genet*. 2009; 5:e1000780. [PubMed: 20019812]
58. Carre-Pierrat M, et al. The SLO-1 BK channel of *Caenorhabditis elegans* is critical for muscle function and is involved in dystrophin-dependent muscle dystrophy. *J Mol Biol*. 2006; 358:387–395. [PubMed: 16527307]
59. Abraham LS, Oh HJ, Sancar F, Richmond JE, Kim H. An alpha-catulin homologue controls neuromuscular function through localization of the dystrophin complex and BK channels in *Caenorhabditis elegans*. *PLoS Genet*. 2010; 6
60. Chen B, et al. α -Catulin CTN-1 is required for BK channel subcellular localization in *C. elegans* body-wall muscle cells. *EMBO J*. 2010; 29:3184–3195. [PubMed: 20700105]
61. Jegla TJ, Zmasek CM, Batalov S, Nayak SK. Evolution of the human ion channel set. *Comb Chem High Throughput Screen*. 2009; 12:2–23. [PubMed: 19149488]
62. Evans, T. WormBook., The *C. elegans* Research Community. WormBook; 2006. Transformation and Microinjection. <http://www.wormbook.org>
63. White JG, Southgate E, Thomson JN, Brenner S. The structure of the nervous system of the nematode *Caenorhabditis elegans*. *Philos Trans R Soc Lond B Biol Sci*. 1986; 314:1–340. [PubMed: 22462104]

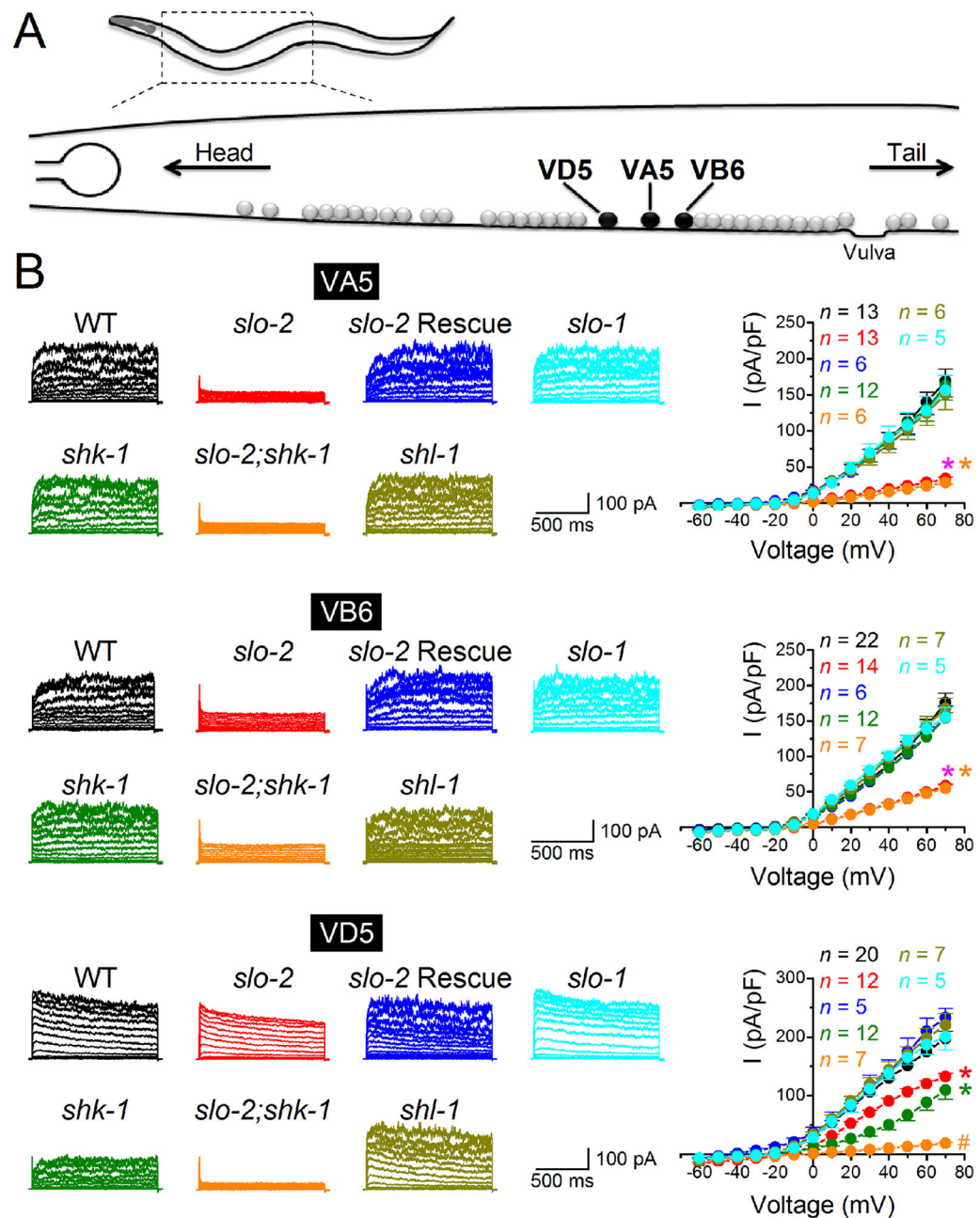


Figure 1.

SLO-2 is an important contributor to delayed outward current in cholinergic and GABAergic motor neurons. **A.** Diagram showing the locations of the recorded motor neurons VD5, VA5 and VB6 (based on published anatomical data⁶³). **B.** Sample whole-cell current traces in response to voltage steps (-60 to +70 mV at 10-mV intervals) from a holding voltage of -60 mV (left) and current-voltage relationships (right) from VA5, VB6 and VD5 of wild type (WT), *slo-2*(*nf101*), *slo-2* rescue, *shk-1*(*ok1581*), *slo-2*(*nf101*);*shk-1*(*ok1581*), *shl-1*(*ok1168*), and *slo-1*(*md1745*). In VA5 and VB6, delayed outward current was greatly decreased in *slo-2*(*nf101*) compared with WT but not further

decreased in the *slo-2;shk-1* double mutant. In VD5, delayed outward current was greatly decreased in both *slo-2(nf101)* and *shk-1(ok1581)*, and was essentially absent in the *slo-2;shk-1* double mutant. Data are shown as mean \pm SE. The asterisk (*) indicates a significant difference compared with WT whereas the pound sign (#) indicates a significant difference compared with the single mutants of *slo-2* and *shk-1* ($p < 0.01$, two-way mixed model ANOVA with Tukey's post hoc tests). The recordings were performed with extracellular solution I and pipette solution I.

Author Manuscript

Author Manuscript

Author Manuscript

Author Manuscript

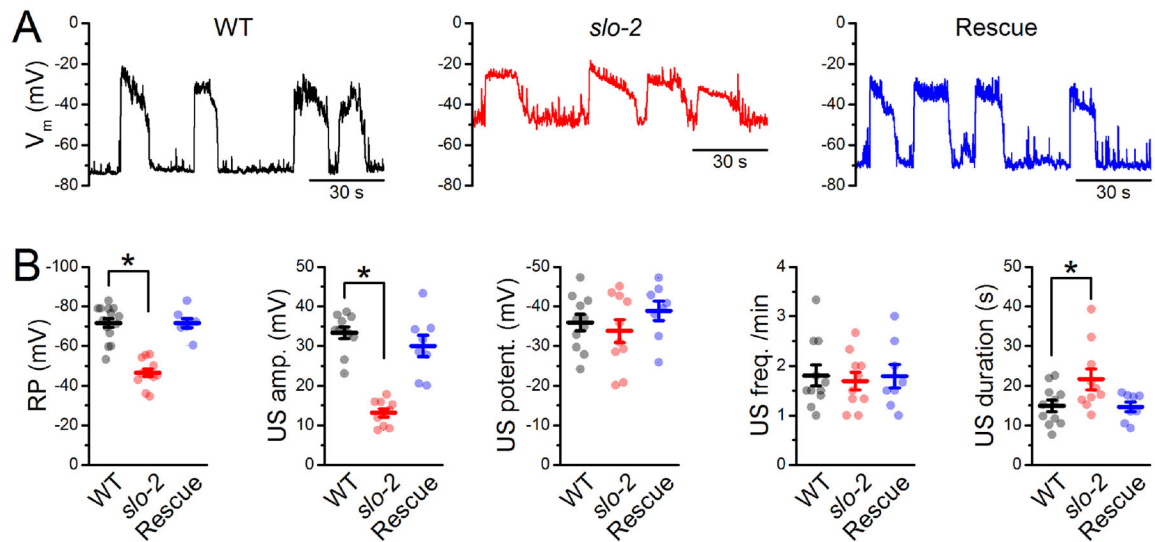


Figure 2.

Loss-of-function mutation of *slo-2* reduced the amplitude of a spontaneous up-state in motor neurons. **A.** Samples traces of spontaneous membrane voltage changes of VA5 from wild type (WT), *slo-2(nf101)*, and *slo-2(nf101)* rescued by expressing wild-type SLO-2b under the control of *Prab-3*. **B.** Comparisons of the resting membrane potential (RP), and up-state (US) frequency, duration, amplitude, and potential. Both the averaged value of each experiment (filled circle) and the mean \pm SE of the group (line and bar) are shown. The asterisk (*) indicates a statistically significant difference compared with WT ($p < 0.05$, one-way ANOVA with Tukey's post hoc tests). The sample size (n) was 15 for WT, 12 for *slo-2*, and 8 for Rescue. Samples without obvious up-states (4 WT and 2 *slo-2* mutant) were not included in the up-state quantifications. The recordings were performed with extracellular solution I and pipette solution I.

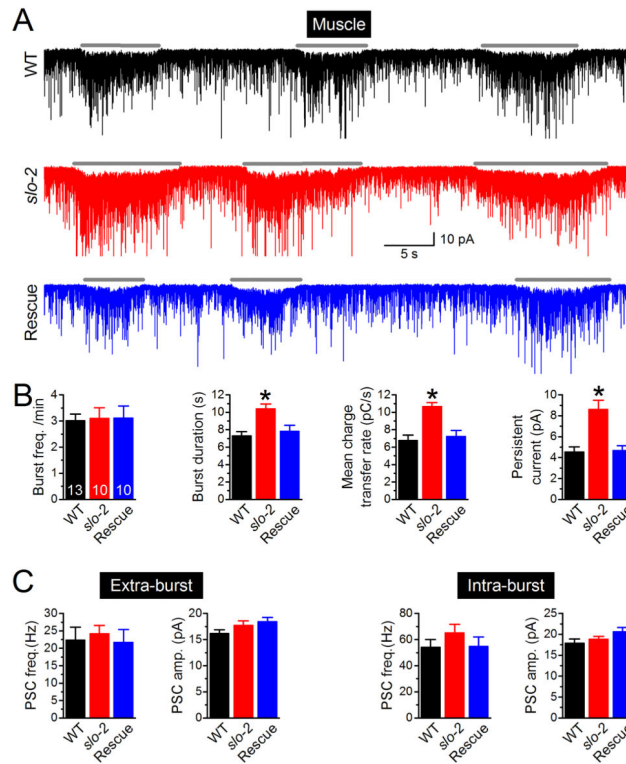
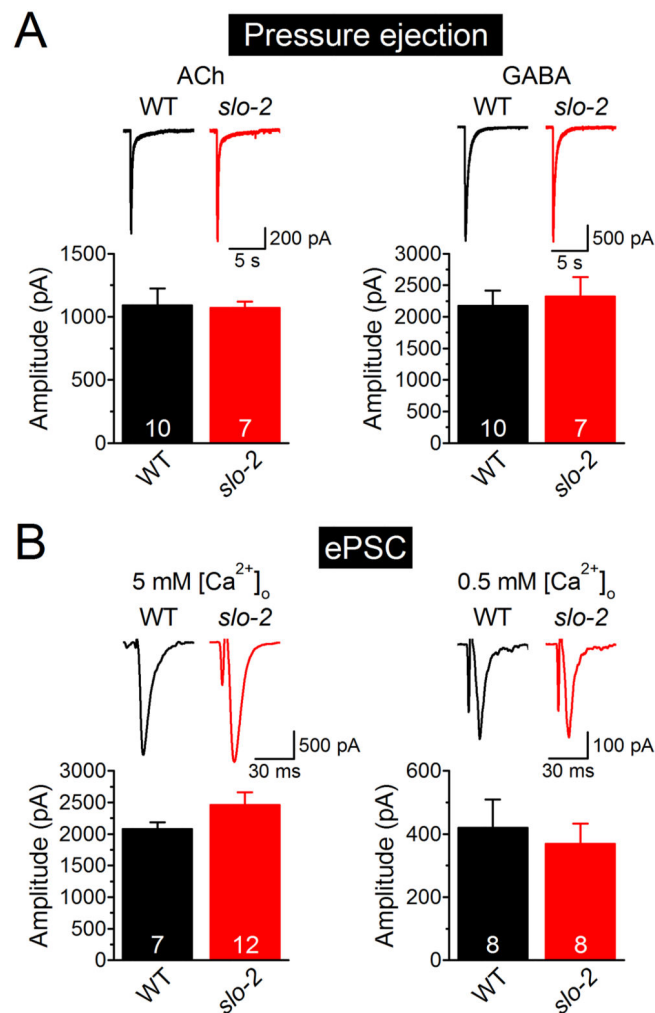


Figure 3. SLO-2 deficiency augmented PSC bursts recorded from body-wall muscle. **A.** Representative traces of spontaneous PSC. The horizontal gray line marks PSC bursts. **B.** Comparison of PSC burst properties. **C.** Comparisons of extra- and intra-burst PSC events. The sample sizes (n) were 17 for wild type (WT), 15 for *slo-2(nf101)*, and 10 for *slo-2(nf101)* expressing *Prab-3::SLO-2::GFP* (Rescue). Data are shown as mean \pm SE. The asterisk (*) indicates a statistically significant difference compared with WT ($p < 0.05$, one-way ANOVA with Tukey's post hoc tests). The recordings were performed with extracellular solution I and pipette solution II.

**Figure 4.**

Postsynaptic receptor sensitivities and ePSCs were normal in *slo-2(nf101)*. **A.** Comparison of muscle cell response to pressure-ejected acetylcholine (ACh, 100 μ M) or GABA (100 μ M) between wild type (WT) and *slo-2(nf101)*. **B.** Comparison of ePSC between WT and *slo-2(nf101)* in the presence of two different extracellular Ca²⁺ concentrations (5 mM and 0.5 mM). Data are shown as mean \pm SE. No significant difference was detected (unpaired *t*-test). The holding voltage was -60 mV in all the experiments. The numbers inside the columns indicate the sample sizes (*n*). All the recordings were performed with pipette solution I. The recordings of ePSC at 0.5 mM [Ca²⁺]_o were performed with extracellular solution II whereas the remaining recordings were recorded with extracellular solution I.

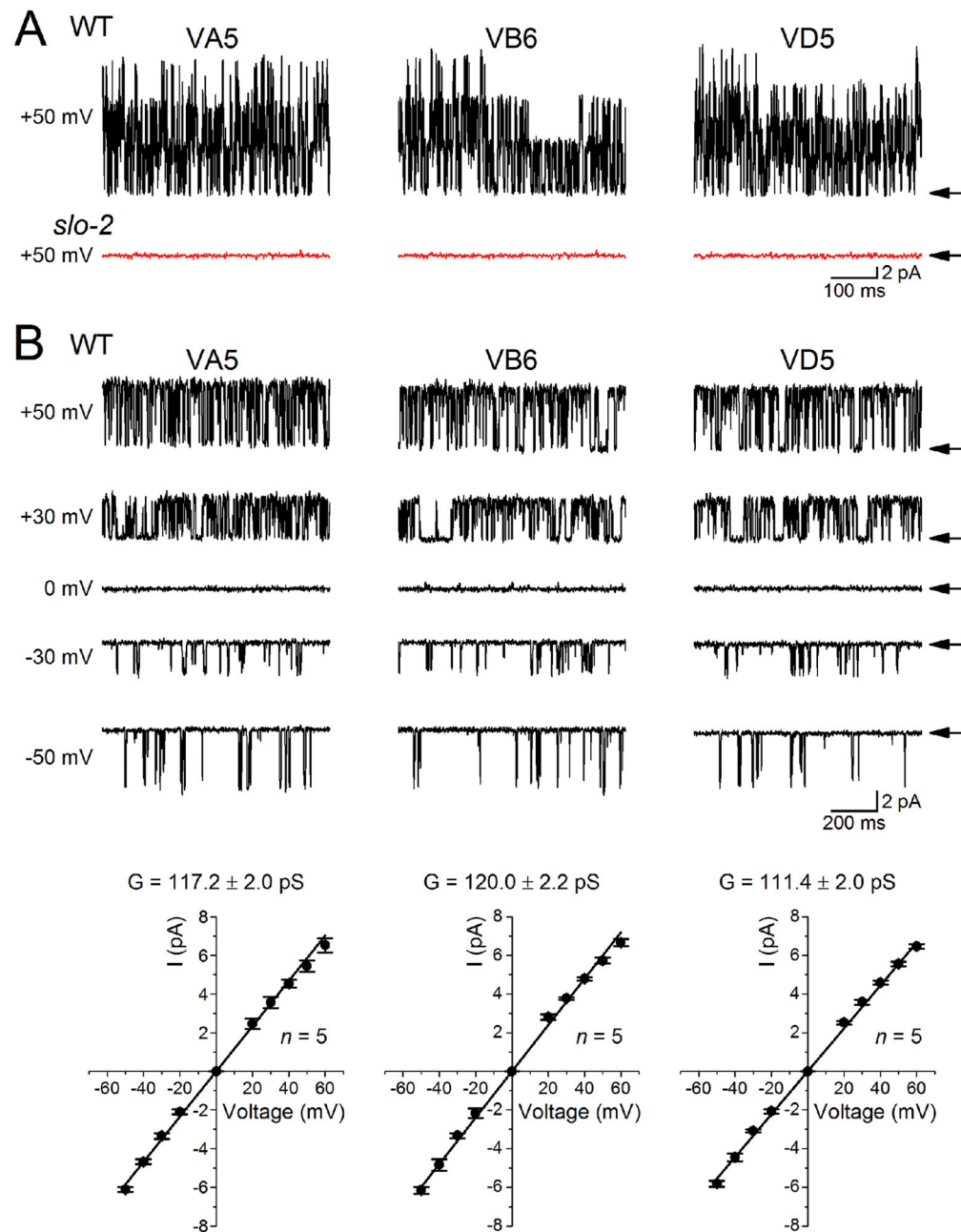


Figure 5. Single-channel conductance of motor neuron SLO-2. **A.** Sample current traces showing SLO-2 single-channel activities in inside-out patches of wild type and the absence of such activities in *slo-2(nf101)*. **B.** Sample SLO-2 single-channel current traces at various membrane voltages from inside-out patches, and the relationship between single-channel current amplitude and holding potential. Data are shown as mean \pm SE. SLO-2 single-channel conductance (G) and sample size (n) are shown in the graphs. For display purpose, the sample traces were chosen from regions where only one channel was open. Arrows mark

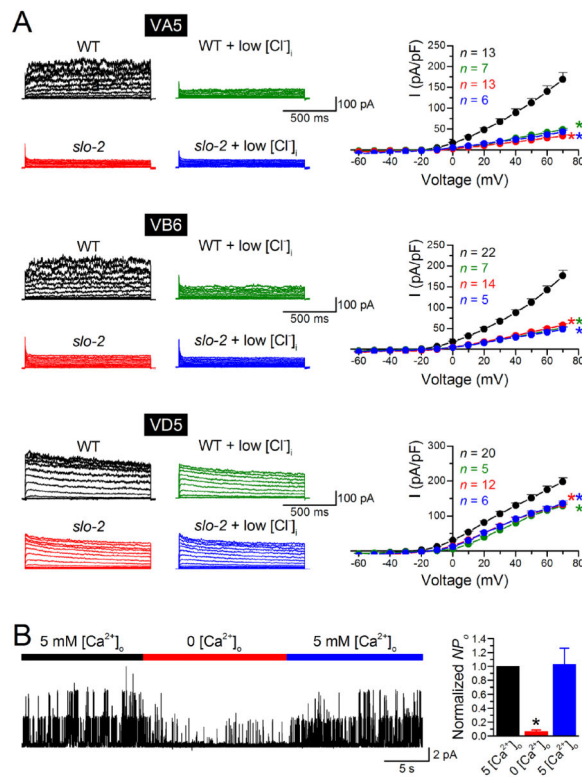
the baseline. The experiments were performed in symmetrical K^+ (pipette solution III and bath solution as specified in Methods).

Author Manuscript

Author Manuscript

Author Manuscript

Author Manuscript

**Figure 6.**

SLO-2 activity in motor neurons depends on cytosolic [Cl⁻] and entry of extracellular Ca²⁺.

A. Whole-cell current traces and relationships between delayed outward current and voltage in representative motor neurons (VA5, VB6 and VD5) of wild type (WT), *slo-2(nf101)*, WT with low [Cl⁻]_i in pipette solution (WT + low [Cl⁻]_i), and *slo-2(nf101)* with low [Cl⁻]_i in pipette solution (*slo-2* + low [Cl⁻]_i) showing that reducing [Cl⁻]_i from the control level (128.5 mM) to a low level (15.3 mM) caused a great reduction of delayed outward current in WT but no change in *slo-2(nf101)*. The asterisk (*) on the right side of a current-voltage relationship indicates a statistically significant ($p < 0.01$) difference compared with WT (two-way mixed model ANOVA with Tukey's posthoc test). All the recordings were performed with extracellular solution I and pipette solution I except for the low [Cl⁻]_i experiments, in which pipette solution II was used instead. **B.** Effects of varying [Ca²⁺]_o on SLO-2 single channel activity in outside-out patches at a holding voltage of +30 mV. The open probability (NP_o) of SLO-2 was normalized to that of the first 5 mM [Ca²⁺]_o period. The asterisk (*) indicates a statistically significant difference compared with the first 5 mM [Ca²⁺]_o period ($p < 0.01$, one-way ANOVA with Tukey's posthoc test, $n = 5$). The recordings were performed with pipette solution I and either extracellular solution I (5 mM Ca²⁺) or extracellular solution III (0 Ca²⁺). In both **A** and **B**, data are shown as mean ± SE.

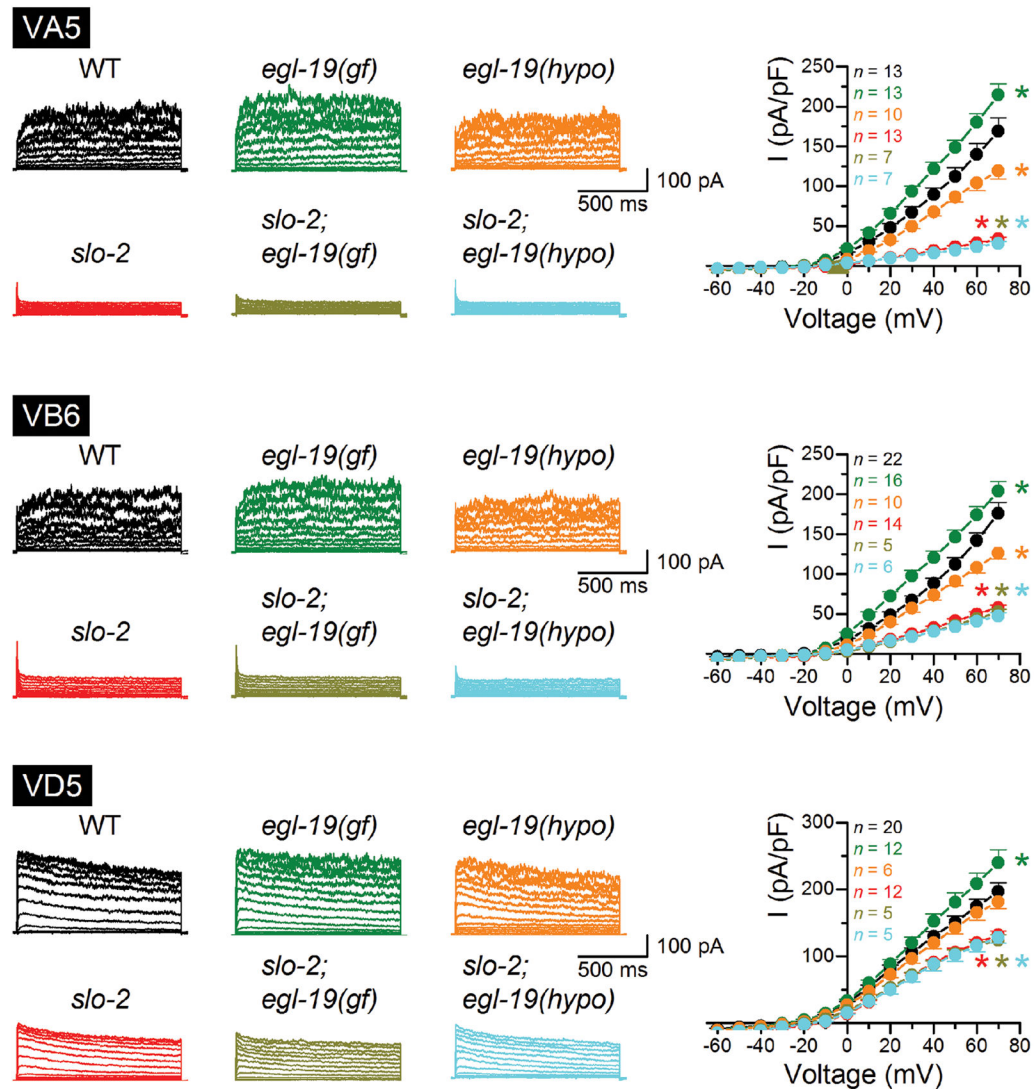
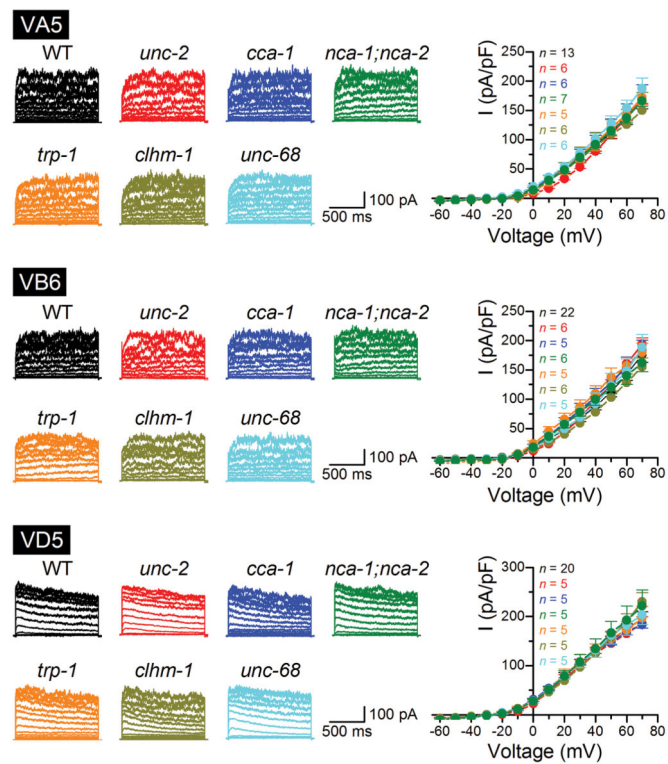


Figure 7.

Mutations of *egl-19* altered delayed outward current of motor neurons in a SLO-2-dependent manner. Whole-cell delayed outward current were recorded from VA5, VB6 and VD5 of wild type (WT), *egl-19(ad695)* (gain-of-function), *egl-19(n582)* (hypomorph), *slo-2(nf101)*, *slo-2(nf101);egl-19(ad695)*; and *slo-2(nf101);egl-19(n582)*. Compared with WT, *egl-19(ad695)* and *egl-19(n582)* augmented and inhibited delayed outward current, respectively, which were not observed in the presence of *slo-2(nf101)*. **Left.** Sample current traces in response to voltage steps (-60 to +70 mV at 10-mV intervals) from a holding potential of -60 mV. **Right.** Current-voltage relationships. Data are shown as mean ± SE. The asterisk (*) indicates a statistically significant difference compared with WT ($p < 0.05$, two-way mixed model ANOVA and Tukey's post hoc tests). The recordings were performed with extracellular solution I and pipette solution I.

**Figure 8.**

Delayed outward current was normal in mutants of other Ca^{2+} channels. Delayed outward currents were unchanged in *unc-2(e55)*, *cca-1(ad1650)*, *trp-1(ok323)*, *clhm-1(ok3617)*, *unc-68(r1162)*, and the double mutant *nca-1(gk9);nca-2(gk5)* compared with wild type (WT) (two-way mixed model ANOVA). **Left.** Sample current traces in response to voltage steps (-60 to $+70$ mV at 10-mV intervals) from a holding potential of -60 mV. **Right.** Current-voltage relationships. Data are shown as mean \pm SE. The recordings were performed with extracellular solution I and pipette solution I.

Table 1

Comparison of the resting membrane potential of motor neurons between wild type and K⁺ channel mutants.

Genotype	VA5	VB6	VD5
Wild type	-71.7 ± 2.4 (n = 15)	-53.2 ± 2.5 (n = 13)	-45.8 ± 1.9 (n = 15)
<i>slo-2</i>	-46.5 ± 2.0 (n = 12)*	-24.0 ± 3.3 (n = 8)*	-25.2 ± 1.6 (n = 12)*
<i>slo-2</i> Rescue	-71.5 ± 2.2 (n = 8)	-48.3 ± 2.1 (n = 6)	-48.2 ± 2.5 (n = 7)
<i>shk-1</i>	-67.9 ± 3.9 (n = 11)	-51.3 ± 2.4 (n = 9)	-42.6 ± 3.2 (n = 6)
<i>slo-2;shk-1</i>	-43.9 ± 2.8 (n = 9)*	-19.9 ± 1.1 (n = 7)*	-20.3 ± 2.4 (n = 6)*
<i>shl-1</i>	-68.0 ± 3.6 (n = 7)	-50.0 ± 3.9 (n = 7)	-48.7 ± 2.6 (n = 5)
<i>slo-1</i>	-69.0 ± 3.0 (n = 9)	-54.9 ± 2.8 (n = 7)	-46.1 ± 2.6 (n = 7)

Data are shown as mean ± SE. An asterisk (*) indicates a statistically significant difference compared with wild type ($p < 0.01$, one-way ANOVA with Tukey's post hoc test).